Research Paper

CAMBRIDGE UNIVERSITY PRESS

A miniaturized CPW-fed CSRR-loaded quad-port MIMO antenna for 5.5/6.5 GHz wireless applications

D. Rajesh Kumar[1] (iD), T. Sangeetha[2], K. G. Sujanth Narayan[3] (iD),
G. Venkat Babu[3] (iD), V. Prithivirajan[1] and M. S. K. Manikandan[4]

[1]Department of Electronics and Communication Engineering, Vel Tech Rangarajan Dr. Sagunthala R&D Institute of Science and Technology, Chennai, Tamilnadu, India; [2]Department of Electronics and Communication Engineering, Karpaga Vinayaga College of Engineering and Technology, Chengalpattu, Tamilnadu, India; [3]Department of Electronics and Communication Engineering, SASTRA Deemed University, Thanjavur, Tamilnadu, India and [4]Department of Electronics and Communication Engineering, Thiagarajar College of Engineering, Madurai, Tamilnadu, India

Abstract

For forthcoming wireless applications, a small and highly decoupled complementary split ring resonators (CSRR)–loaded co-planar waveguide (CPW)–fed antenna for dual-band applications is investigated. The low-profile antenna consists of a CSRR-loaded rectangular radiating element with a truncated bottom, giving a wideband performance over the frequency ranges of 5.28–5.52 GHz and 6–7.2 GHz. The antenna has been printed on a widely used FR4 substrate measuring $7.5 \times 10.5 \times 1.6$ mm^3 in volume. This research's suggested antenna is turned into a 4×4 multi input multi output (MIMO) construction using a 25×25 mm^2 printed circuit board. Individual antennas were isolated by nearly 20 dB without using a decoupling device. The antenna has been built, and the measured and simulated results correspond well. Computing envelope correlation coefficient (ECC), channel capacity (CC), and channel capacity loss (CCL) further validates the antenna's performance (–). The antenna has an overall gain of around 2.54 dBi and a radiation efficiency of approximately 89% throughout the relevant spectral range, which is much better for wireless applications. The suggested antenna's omnidirectional emission pattern makes it a potential contender for future wireless and cellular applications.

Introduction

Wireless communication has grown nearly linearly since the start of the 21st century. The vehicle-to-vehicle communication, autonomous vehicles, and health care applications are examples of mobile communication systems that are regarded as industry standards. Wi-Fi or Bluetooth networks, GPS, satellite communication, and other technologies serve as various foundations for modern wireless communication systems. In an effort to fit as many operations into a single device as feasible, researchers and engineers have a propensity to merge many tasks into one. This is done to create devices that are both compact and clever. It is inconceivable to imagine a wireless communication system without an antenna. So, antennas need to be made in a way that lets them work well for many different applications at the same time. Because of this pattern, there has been a big rise in interest in multiband or broadband printed antennas in the last few years. Since multiband antennas can keep their different frequencies from interfering with each other, the front end of a system that uses them can be made simpler. Traditional ways to get multiband frequency response include stacking patches, using antennas with defective ground planes [1–5], making slots in patches [6–8], and using fractal configuration, among other things. In multilayer patch antennas, radiating elements at the bottom are fed, while all other patches work as "parasitic patches." This makes the connection between the two resonant patches weak, which lets them work at two different frequencies. Long and Walter [9] were the first scientists to talk about the results of experiments with this kind of setup. The biggest problem with this kind of layout is that it might be hard to get all of the layers to line up right. The layout of parasite patches is also a big problem that needs to be solved. Adding a slot to the patch is another option that could be used to reach the goal of getting multiple frequency bands. Most of the time, the resonance frequency of slots is different from that of the patch. Adding a slot could cause an extra resonance to happen. The latest trend in building multiband patch antennas is to use fractal geometry. Fractal patch antennas can use many different fractal shapes to get the best performance.

In the past, many multi input multi output (MIMO) antenna systems with a single band [10–17] and dual band [18] were made for a wide range of wireless uses: a wideband MIMO
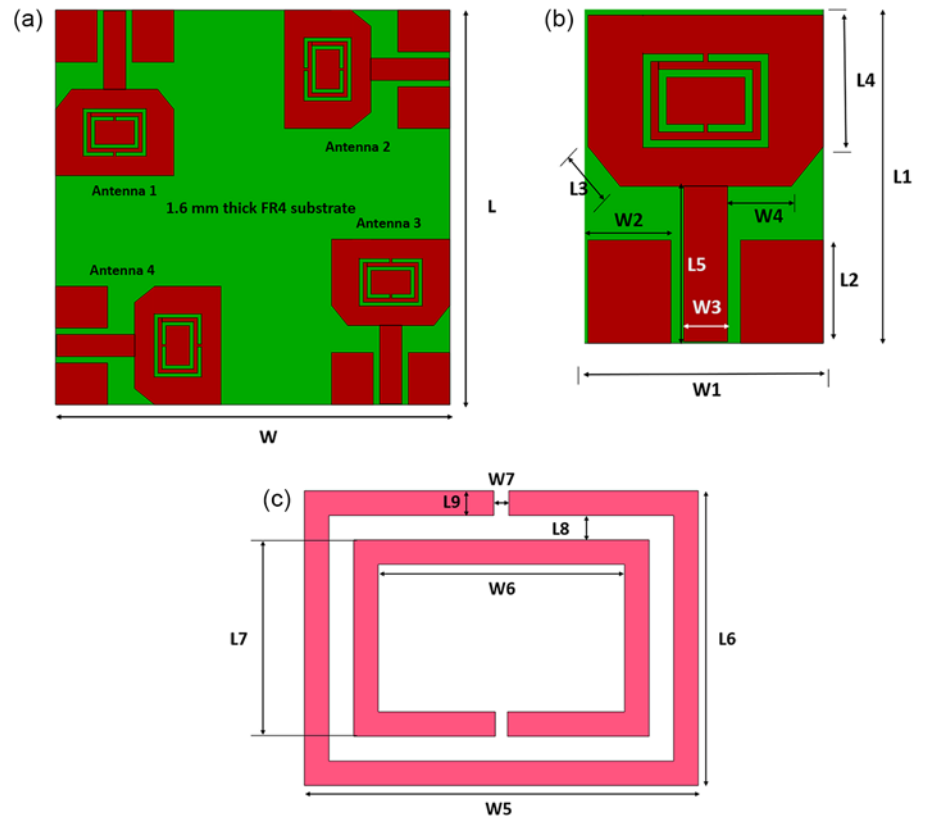
Figure 1. (a) Structure of Single antenna element, (b) Schematic representation of proposed CPW antenna, (c) structure of CSRR.

antenna for wireless LAN applications [19], two concentric slot-based MIMO for 4G/5G mobile phones [20], complementary split ring resonators (CSRR)–loaded multiband antennas with high isolation and higher order mode suppression [21, 22]. Compared to the standard patch antennas, these designs are smaller and can work over a wider range of frequencies. The biggest problem with fractal geometries is that it might be hard to make the complicated shapes with a lot of accuracy. Using metamaterials is a better way to make patch antennas that can work with more than one band. Researchers from different places have come up with different models for multiband patch antennas that are based on metamaterials. presents a study in which the authorsAn introductory phrase seems to be missing in the sentence "presents a study in which the authors put split ring resonators on a printed dipole (SRR). In [23], the authors showed a different way to make multiple resonance patch antennas with split ring resonator printed over top of the antennas. One more report of a multiband dipole was made in [24]. The authors used CSRR to make multiband work. In [25], a CLRH transmission line–based antenna is suggested. Depending on how it is being used, it can vibrate at different frequencies. Within the scope of this study, a new way to make multiband antennas is proposed by putting metamaterial CSRR into the antenna's structure. A patch antenna with CSRR on it is held up by the ground plane. This is what the antenna is made out of. CSRRs can make more than one resonant frequency, depending on how big they are and how far apart they are. There are three bands on this antenna, and two of them can be used for wireless local area networks and fixed satellite services.

Here, we have presented a miniaturized four-port CSRR-loaded MIMO antenna for 5.5 and 6.5 GHz applications. The context of the article is broken into four phases. Phase 1 discusses design methodology and analysis with constructional details of the

Table 1. Various dimensional parameters of proposed antenna.

Parameters	L	W	L1	W1	L2	W2	L3	W3
Values (mm)	25	25	10.435	7.5	3.3	2.64	1.02	1.4
L4	W4	L5	W5	L6	W6	L7	W7	L8	L9
4.2	2.03	4.9	4	3	2.5	2	0.15	0.245	0.245

antenna. Various simulated results including S-parameters, parametric study, current distribution, and polarization diversity have been explained in detail in Phase II of the paper. Then Phase III focuses on measured results with fabricated prototype of the proposed MIMO antenna. Finally, various MIMO parameters have been taken into account and analyzed in detail with suitable graphs in Phase IV.

Main contributions of this research could be stated as follows:

1. A miniaturized dual-band MIMO antenna presented with overall size 25×25 mm^2, which is significantly small and highly suitable for IoT applications.
2. Individual antenna contributes to total area of size 10.485×7.5 mm^2, with wideband operations ranging from 6.1 to 6.9 GHz (second band).
3. With this small volume of size, the proposed antenna is able to offer substantial isolation better than 25 dB, thereby enhancing other overall MIMO performance.
4. In addition, a decoupling mechanism has not been included and because of this, the general configuration of the antenna has been kept as simple as possible.
5. Polarization diversity has been achieved after placing antenna elements over different corners of the substrate.
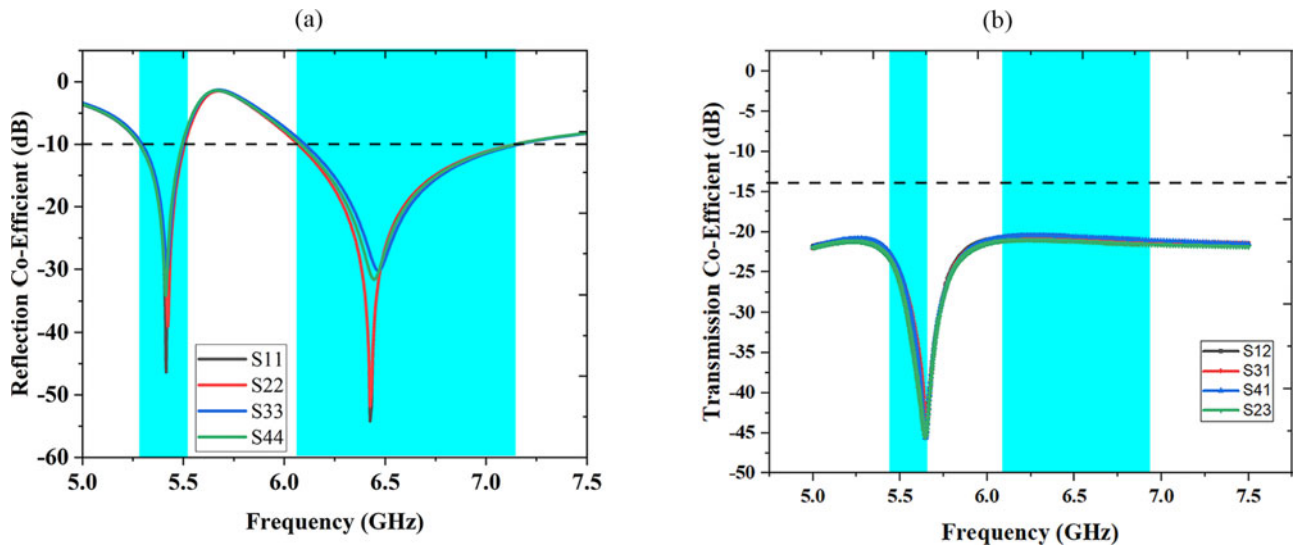
Figure 2. (a) S_{ii} of Antenna 1-4, (b) S_{ij} of 4-port CSRR loaded antenna.
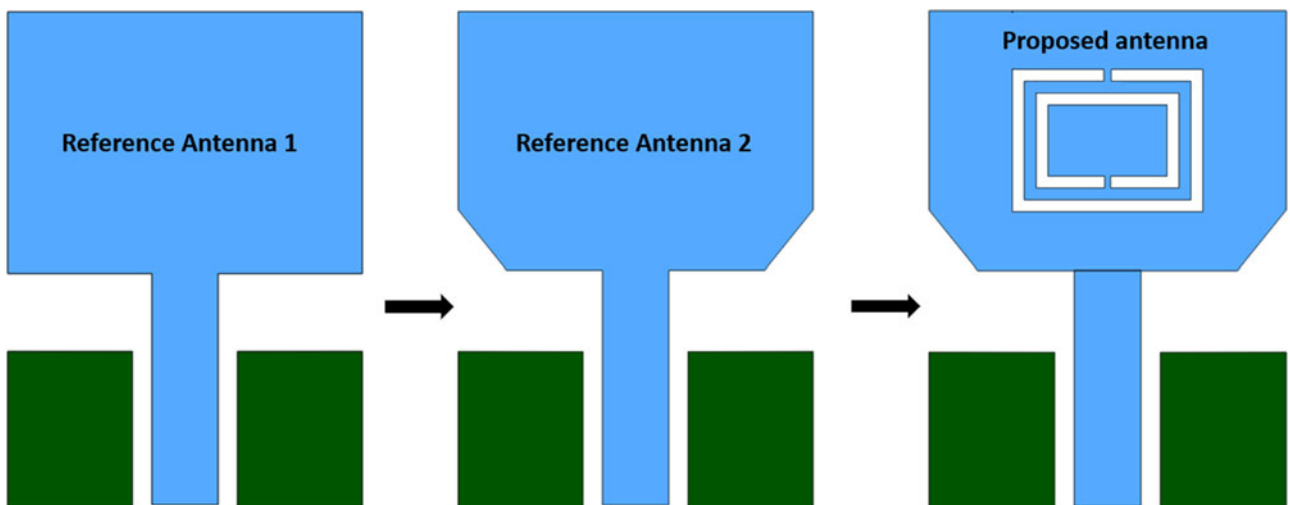

Figure 3. Evolution of 4-port CSRR loaded antenna.

Design and investigation of MIMO antenna

The proposed four-port CSRR-loaded wideband truncated co-planar waveguide (CPW) antenna for dual-band applications is illustrated in Fig. 1(a). The proposed four-port truncated antenna is designed on 25×25 mm^2 widely used FR4 substrate with thickness 1.6 mm. As the proposed antenna employs CPW structure, the ground plane has been printed on top side of the substrate with dimension 2.64×3.3 mm^2. The proposed antenna consists of truncated rectangular radiator of size 7.5×5.47 mm^2, which is fed by 1.4×4.98 mm^2-sized feeding element. At the center of the truncated radiator, rectangular-shaped CSRR slot is etched to produce additional resonance. Structure and dimension detail of the four-port antenna are illustrated in Fig. 1(a), and constructional details of Antenna 1 is depicted in Fig. 1(b).

All CSRR-loaded antennas are positioned at four corners of the substrate in order to achieve high isolation and pattern diversity features. The dimensional details of CSRR structure are depicted in Fig. 1(c). CSRR structure is made up of rectangular strip of width 1 mm with outer and inner square ring area of $L6 \times W5$ mm^2 and

$L7 \times W6$ mm^2, respectively. Both the outer and inner rings have space at edges of size W7 mm. Table 1 listed the values of various dimensions of the single-element truncated Wi-Fi 6E antenna elements. All dimensions have been finalized after performing parametric analysis using Keysight's Advanced Design System Software. All the values given in Table 1 measures in millimeters.

It is observed that all the antenna elements in the MIMO system cover dual-band frequency spectrum spanning from 5.28 to 5.52 GHz and 6.1 to 6.9 GHz, respectively, over 10 dB impedance bandwidth as shown in Fig. 2(a). On the other hand, transmission coefficient of four-port antenna system is shown in Fig. 2(b). Isolation among antenna system is achieved up to 12.5 dB by placing each antenna in orthogonal fashion. One more advantage with orthogonal placement is that it is not necessary to concentrate on decoupling mechanism.

Evolution stages of the proposed antenna is illustrated in Fig. 3. Initially, the proposed antenna consists of a rectangular element as main radiator named here as Reference Antenna 1. As depicted in Fig. 4, Reference Antenna 1 has single-band resonance ranging
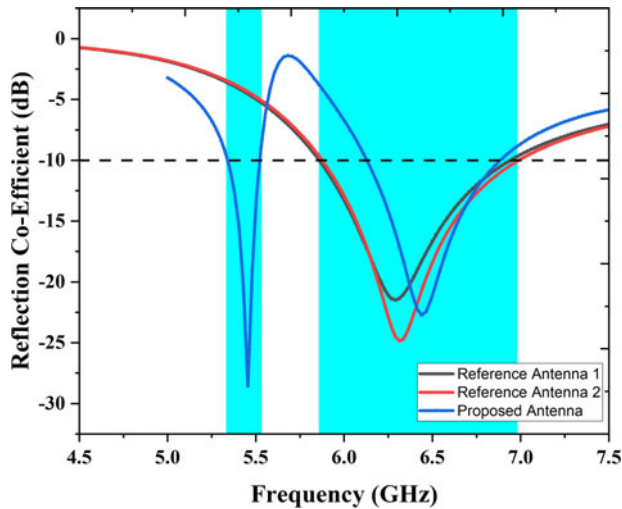
**Figure 4.** Reflection Co-Efficient of Evolution stages.

from 5.8 to 7 GHz over 10 dB impedance bandwidth. The bottom edges of the Reference Antenna 1 has been truncated as shown in Fig. 3 (Reference Antenna 2), which improves impedance matching beyond 25 dB with same frequency of operation as Reference Antenna 1. CSRR structure has been incorporated as slot at the center of Reference Antenna 2 to get additional resonance at 5.3–5.6 GHz with reflection coefficient less than 10 dB.

Parametric analysis

When L4 = 3.2 as a result of L4's impact on the frequency of operation at the intended spectrum, changes have been seen in both bands as illustrated in Fig. 5(a). It should come as no surprise that as the length of the antenna rose, the frequency of operation dropped. Similar responses were seen when the feed length (L5) was gradually increased from 3.9 to 5.9 mm in increments of 1 mm. On the other hand, the impedance matching of the antenna in dual-band response is determined, as illustrated in Fig. 5(b), by the feed length.

Finally, the length of the ground plane (L2) is changed from 1.3 to 4.3 mm, and it is seen that when L2 is decreased, both the lower band responses and the higher band responses are entirely impaired as shown in Fig. 5(c). Surface current visualizations demonstrate the unique roles played by various CSRRs in relation to various resonances. For low frequency band, maximum current distribution is observed over top edge of radiating patch along with edges of CSRR as shown in Fig. 6(a). However, at 6.5 GHz, the overall length of electrical path is completely shrunk by attaining maximum current only around inner edge of CSRR as shown in Fig. 6(b). When Antenna 1 is excited, the surface current distributions are as shown in Fig. 7(a) and (b), respectively, at frequencies of 5.5 and 6.5 GHz. It is clear that when antenna 1 is stimulated, the other antennas are virtually entirely isolated, which results in an improvement in isolation of more than 20 dB.

A simulated three-dimensional radiation pattern is shown in Figure 8. This pattern contributes to an understanding of the polarization variety. When Antenna 1 (aligned on the *x*-axis) is triggered, the greatest amount of radiation travels in the direction of +*y* for both bands. However, when Antenna 2 (aligned on the *y*-axis) is stimulated for both bands, the highest radiation
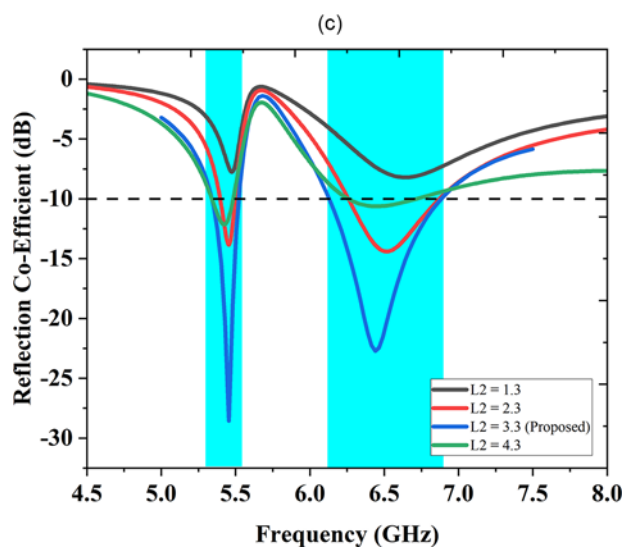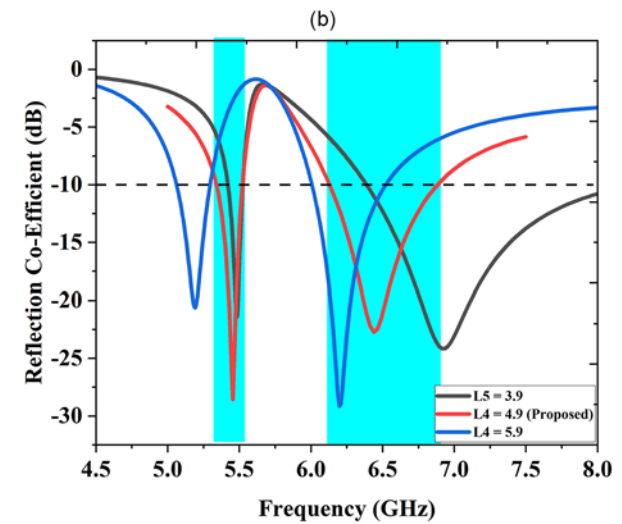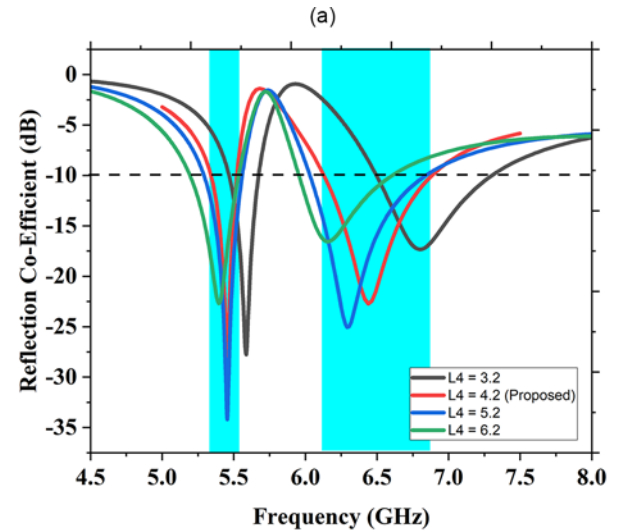
Figure 5. Parametric Study on parameters (a) L4, (b) L5, (c) L2.

occurs in the positive *x* direction. The same scenario is observed for Antenna 3 and Antenna 4 as well. Therefore, polarization diversity
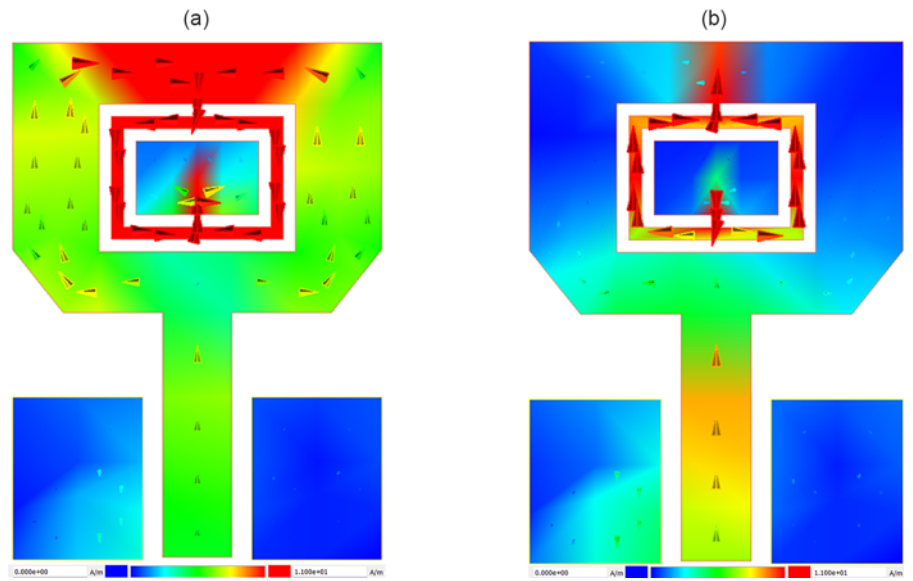
Figure 6. Surface Current distribution of Antenna 1 at (a) 5.5 GHz, (b) 6.5 GHz.
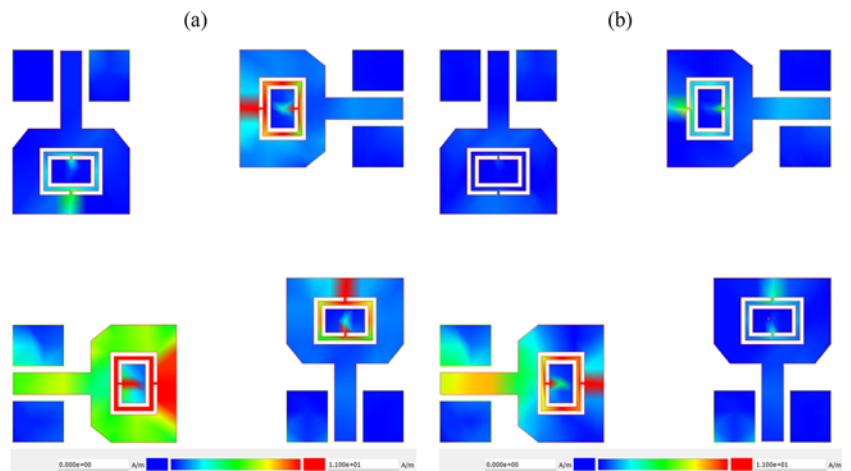
Figure 7. Current distribution of MIMO antenna at (a) 5.5 GHz, (b) 6.5 GHz.

Figure 8. 3-D Radiation pattern of Proposed antenna.

may be accomplished by positioning the antennas in a manner that is distinct from one another relative to one another, which results in improved isolation.

Measured results and discussions

It has been successfully accomplished to manufacture the prototype of the suggested four-port CSRR-loaded truncated

Figure 9. Fabricated prototype of CSRR loaded MIMO antenna.

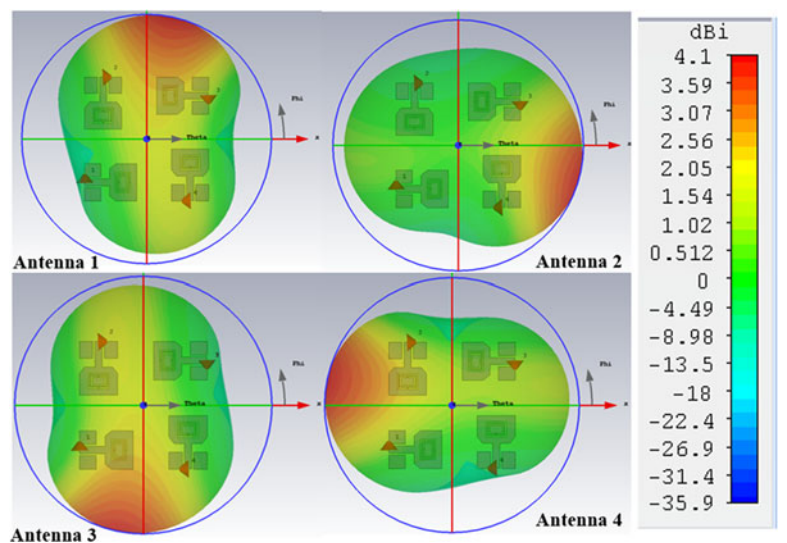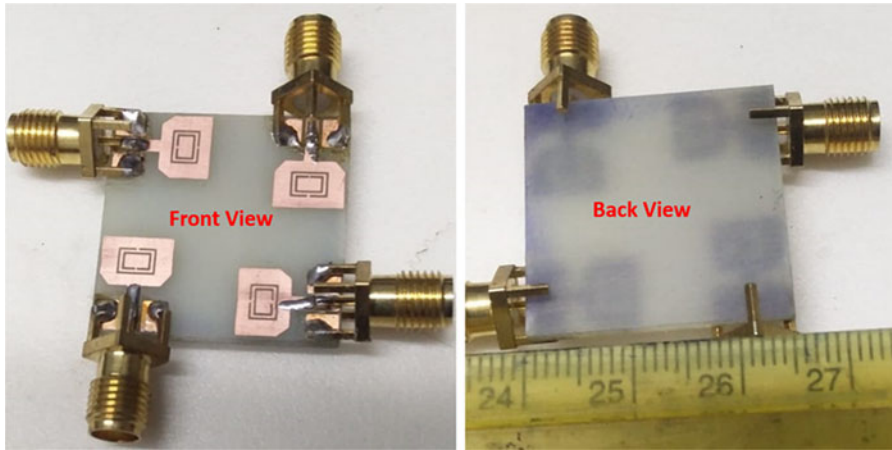antenna, and it has been successfully accomplished to test the usual antenna parameters in practice. Both the top and bottom views of the manufactured antenna are shown in Fig. 9. During measurements, 50-ohm terminator is used at all SMA connectors except at the antenna for which measurement is to be carried out. Using Keysight's Firefox Network Analyzer, S-parameters, also known as reflection and transmission coefficient, are measured and displayed in the manner seen in Fig. 10(a) and (b). It is profusely clear that the findings of the measurements have a strong correlation with the results of the simulations, which encompass two desirable bands of operations. There is often very little fluctuation in the findings of the measurements, and this is typically because of variations in the dielectric constant of the substrate as well as conducting losses caused by the effects of soldering.

Two-dimensional radiation pattern of CSRR-loaded antenna is presented as shown in Fig. 11(a–d) at 5.5 and 6.5 GHz for phi = 0° and phi = 90°. It shows that the proposed antenna yields bidirectional radiation pattern for co-polarization of both the resonance and achieves cross-polarization less than 30 dB for required bands of operation. Furthermore, it is noticed that both simulated and measured patterns are well correlated with each other.

Figure 12 demonstrates that the CSRR-loaded antenna obtains a significant gain of roughly 2–2.3 dB across the operational bandwidth. This demonstrates that the suggested antenna is very appropriate for future wireless applications.

MIMO performance

When it comes to determining how isolated one channel is from the others in a communication system with several channels, envelope correlation coefficient (ECC) is a crucial statistic to use. When the value is lowered, the antenna demonstrates a better MIMO performance. The ECCs that were generated in order to assess the performance of the proposed MIMO antenna using the observed S-parameters and equation (1) are shown in Fig. 13(a).

$$ECC = \frac{\left| Smm^{*}Smn + Snm^{*}Snn \right|^{2}}{\left(1 - |Smm|^{2} - |Smn|^{2} \right)\left(1 - |Snm|^{2} - |Snn|^{2} \right)}. \quad (1)$$

All of the ECC values in the frequency ranges that are acceptable are lower than 0.035 as shown in Fig. 13(a), which indicates that the performance is rather satisfactory overall. When compared
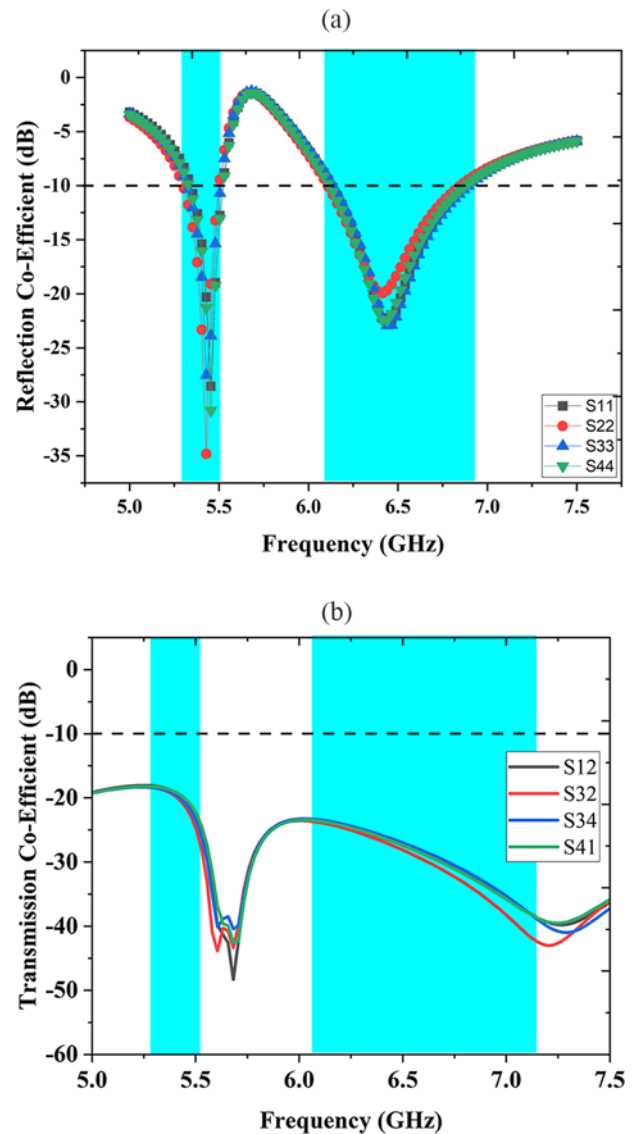
Figure 10. Measured (a) Reflection Co-Efficient, (b) Transmission Co-Efficient.

to a single antenna, the signal-to-noise ratio of the system may be improved with the use of diversity scenario, which is provided by a
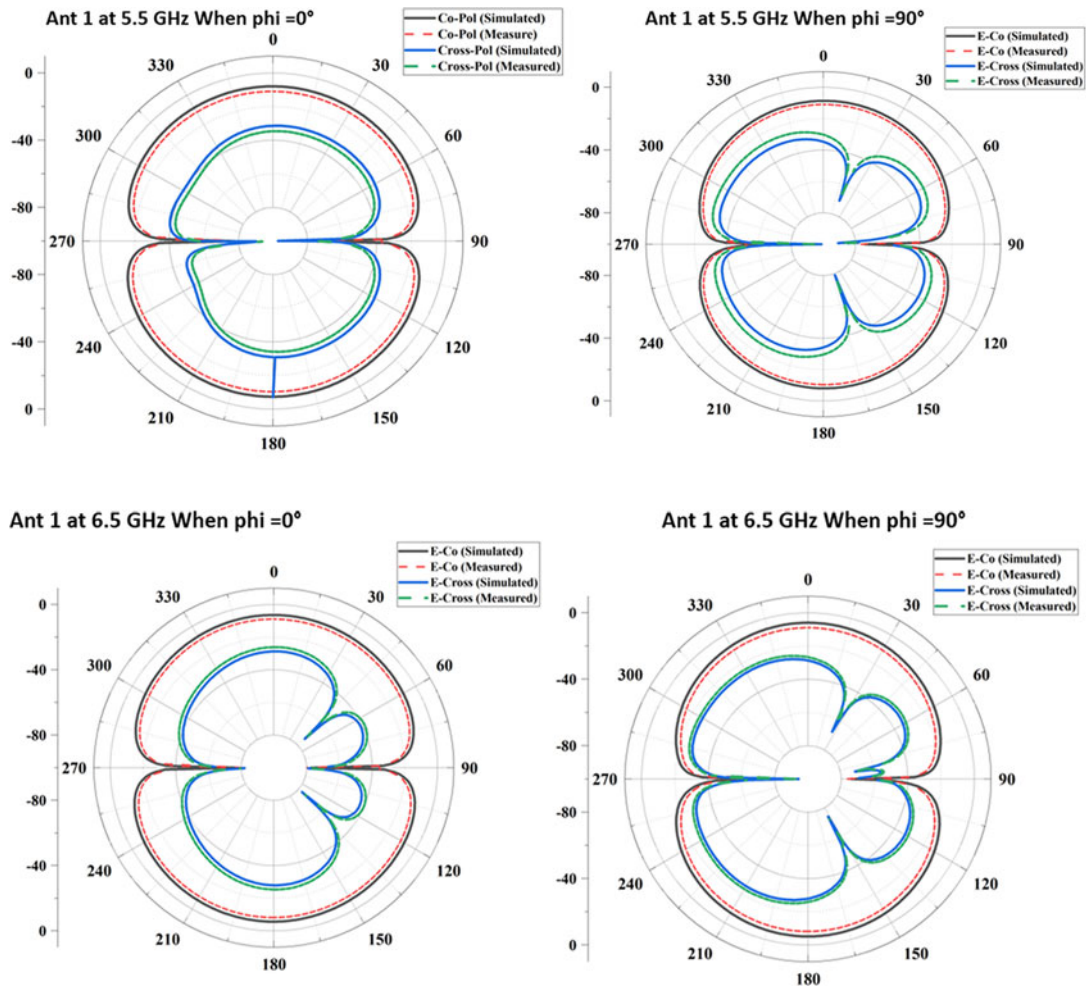
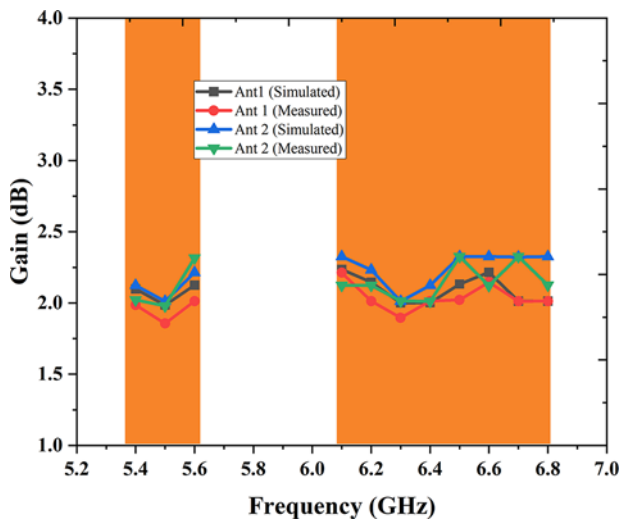**Figure 11.** Two-Dimensional Radiation Pattern of antenna 1.

Figure 12. Gain of the proposed antenna.

MIMO antenna. The diversity gain (DG) is a measure that may be used to determine the level of improvement in the signal-to-noise ratio. The answer to the question of how to ascertain the outcome

of DG's calculation using ECC may be found in equation (2) and plotted in Fig. 13(b).

$$\text{Diversity Gain } (i,j) = \sqrt{1 - \text{ECC}_{i,j}} \tag{2}$$

In addition to this, we analyze the channel capacity loss (CCL), which is often referred to as CLL of the MIMO antenna. CLL is an essential data transmission rate parameter that is computed mathematically using equation (3).

$$\text{Channel Loss } (\text{CL}) = -\log_2 \det\left(\varphi^R\right) \tag{3}$$

$$\varphi^R = \begin{bmatrix} p_{11} & \cdots & p_{14} \\ \vdots & \ddots & \vdots \\ p_{41} & \cdots & p_{44} \end{bmatrix} \tag{4}$$

where

$$p_{ii} = 1 - \left(\left(S_{ii}^2\right) + \left(S_{ij}^2\right)\right)$$

$$p_{ij} = -\left(S_{ii}^* S_{ij} + S_{ji}^* S_{jj}\right) \text{ for } i,j = 1,2,\ldots,4.$$

The calculated and observed CCL of the suggested antenna is shown in Fig. 13(d). The whole spectrum maintains an acceptable CLL value of less than 0.4 bits/sec/Hz, which is consistent with the results of CLL simulations and guarantees adequate data transmission rates in MIMO systems. Furthermore, channel capacity (CC)
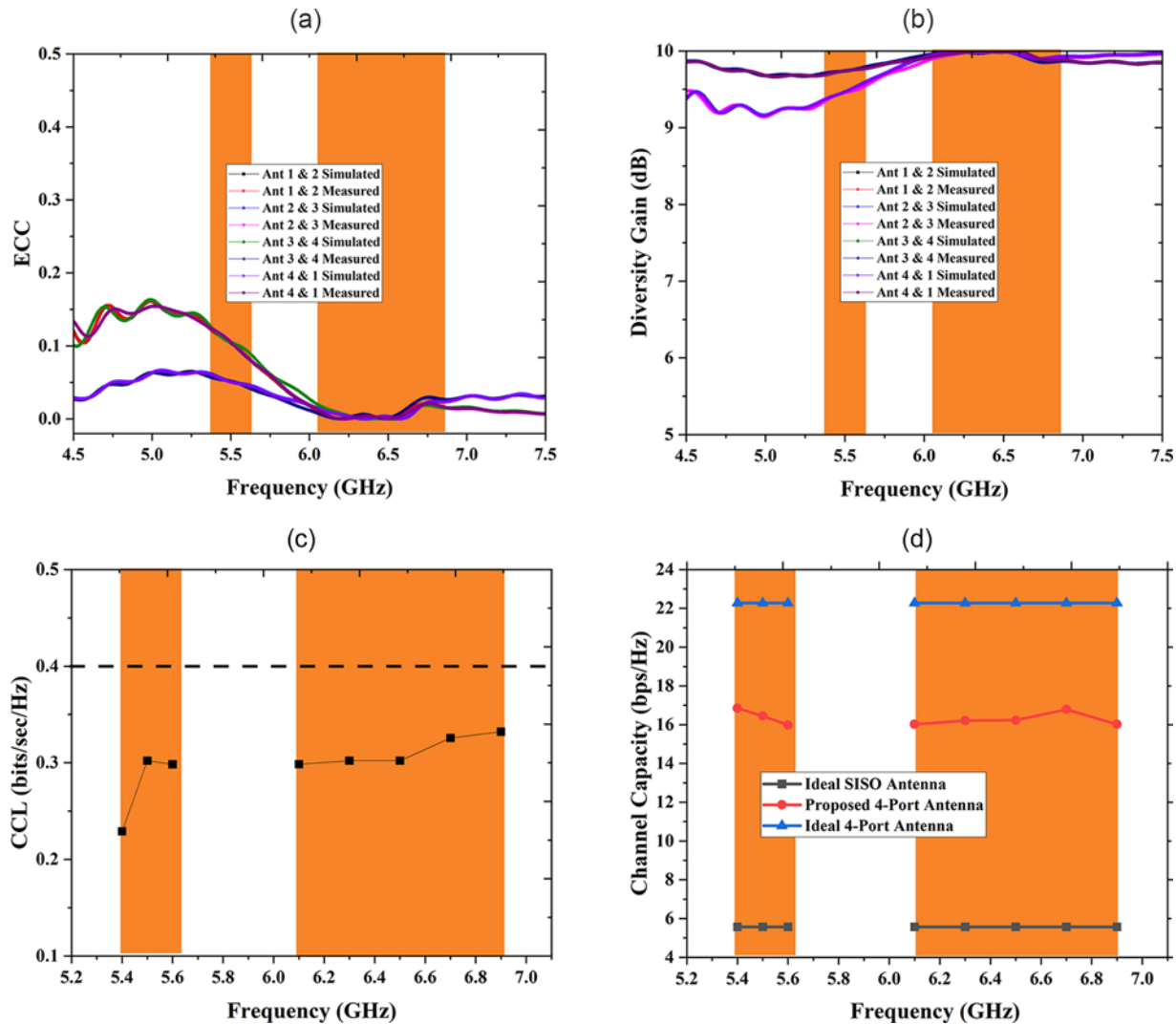
Figure 13. (a) Envelope Correlation Co-efficient, (b) Diversity Gain, (c) Calculated Channel Capacity Loss, (d) Channel Capacity.

is an important parameter to be calculated to validate the MIMO performance. Therefore, CC has been calculated from simulated efficiencies of individual antenna elements by considering 20 dB signal-to-noise ratio environment.

For ideal single input single output antenna, CC is around 5.57 bps/Hz, whereas for ideal 4×4 MIMO antenna, it is around 22.28 bps/Hz. It is calculated that CC for the proposed CSRR-loaded four-port antenna is around 16.68 bps/Hz over required band of operation as illustrated in Fig. 13(d). In conclusion, it is evident that the constructed antenna beats all essential MIMO measures, such as ECC, DG, CLL, and CC.

A detailed comparison is provided in Table 2 to evaluate how the proposed antenna stands apart from other MIMO antennas discussed in the literature. A total of six features have been taken into account and compared with existing antennas. It has apparently been shown that the overall dimension of the proposed antenna is very small in comparison with other antennas. Our antenna occupies a total area of 25×25 mm^2, with an individual antenna size of 10.485×7.5 mm^2, which is significantly smaller than any other antenna in the literature. It is obvious that isolation is the major concern while designing MIMO antennas because

the distance between antenna elements should be as great as possible. The greater the separation between antenna elements, the better the isolation, and vice versa. Even after placing antenna elements in a small area, the proposed MIMO antenna is still able to offer isolation better than 25 dB. In addition to that, no decoupling mechanism has been incorporated for enhancing isolation. Then, most of the antennas described in the literature are able to offer single-band operation, whereas the proposed CSRR-loaded antenna provides dual-band resonance at 5.5 and 6.5 GHz. The proposed MIMO antenna has ECCs less than 0.1 and an overall gain of around 2.5 dB in the desired band of operation. The above comparison enables us to understand how the antenna presented in this work stands out from other works in the literature.

Conclusion

A very compact CSRR-loaded four-port antenna for dual band (5.5/6.5 GHz) applications has been successfully investigated. The major advantage of the proposed antenna is found on its overall reduced dimension of size 25×25 mm^2 with enhanced isolation beyond 25 dB. The antenna design process is explained in

Table 2. Performance measure of proposed MIMO antenna with existing antennas.

S. No.	MIMO antenna size	MIMO antenna size in terms of wavelength (λ)	Individual antenna size (mm^2)	Individual antenna size in terms of wavelength (λ)	Isolation (dB)	Operating frequency (GHz)	Dual band achieved	ECC	Gain (dB)
[10]	60 × 90	0.49λ × 0.735λ	17 × 21	0.138λ × 0.1715λ	18	2.45	No	NA	0.55
[11]	100 × 50	0.816λ × 0.408λ	18 × 14	0.147λ × 0.1143λ	10	2.45	No	NA	NA
[12]	61 × 61	0.498λ × 0.498λ	–	–	28	2.45	No	<0.3	3.8
[13]	60 × 60	0.49λ × 0.498λ	–	–	22	2.45	No	<0.4	3.4
[14]	42 × 42	0.77λ × 0.77λ	22 × 16	0.403λ × 0.293λ	10	5.5	No	NA	5
[15]	140 × 120	1.09λ × 0.94λ	15.5 × 8	0.121λ × 0.062λ	15	2.35	No	NA	NA
[17]	40 × 40	0.446λ × 0.446λ	27 × 18	0.3015λ × 0.201λ	10	3.35	No	NA	7.9
[19]	50 × 50	0.408λ × 0.408λ	–	–	17.5	2.45	No	<0.5	2.1
[20]	100 × 60	0.703λ × 0.422λ	15 × 8	0.1055λ × 0.056λ	NA	2.119 and 17.55	Yes	0.04	8
[21]	60 × 60	0.49λ × 0.49λ	22 × 17	0.179λ × 0.138λ	17	0.875, 1.75, 1.82, 2, 2.45	Yes	<0.05	−2
[22]	52 × 52	0.676λ × 0.676λ	20 × 20	0.26λ × 0.26λ	20	3.4 and 3.9	Yes	<0.5	6
Proposed	25 × 25	0.54λ × 0.54λ	10.485 × 7.5	0.22λ × 0.1625λ	25	5.5 and 6.5	Yes	<0.1	2.2−2.5

detail with evolution stages of the antenna followed by parametric analysis. Increased isolation is achieved by placing all antenna elements over different corner of FR4 substrate, thereby achieving pattern diversity. In order to validate the performance, the proposed antenna is fabricated and various parameters are measured, which reveals that measured parameters are well correlated with simulated results. Furthermore, MIMO parameters such as ECC, CCL, DG, and CC have been computed from the simulated and measured results. It is noticed that ECCs of MIMO antenna is lower than 0.1 over the operating spectrums with CC loss below 0.4. Then, diversity gain around 9.5 dB is achieved with CC of 16.68 bps/Hz. The results clearly show that the MIMO antenna presented in this article could be a viable choice for various wireless applications.

Competing interest. There is no conflict of interest between authors.

References

1. **Kuo YL and Wong KL** (2003) Printed double-T monopole antenna for 2.4/5.2 GHz dual-band WLAN operations. *IEEE Transactions on Antennas and Propagation* **51**(9), 2187–2192.
2. **Liu WC, Chen WR and Wu CM** (2004) Printed double S-shaped monopole antenna for wideband and multiband operation of wireless communications. *IEE Proceedings—Microwaves, Antennas and Propagation* **151**(6), 473–476.
3. **Ammann MJ and Farrell R** (2005) Dual-band monopole antenna with stagger-tuned arms for broad banding. In *IEEE International Workshop on Antenna Technology*, 278–281.
4. **John M and Ammann MJ** (2006) Integrated antenna for multiband multinational wireless combined with GSM1800/PCS1900/IMT200 extension. *Microwave and Optical Technology Letters* **48**(3), 613–615.
5. **Ge Y, Esselle KP and Bird TS** (2006) Compact triple-band multiband monopole antenna. *International Workshop on Antenna Technology* **1**, 172–175.
6. **Wang H** (2006) Dual-resonance monopole antenna with tuning stubs. *IEE Proceedings—Microwaves, Antennas and Propagation* **153**(4), 395–399.
7. **Wang H and Zheng M** (2008) Triple-band wireless local area network monopole antenna. *IET Microwaves, Antennas & Propagation* **2**(4), 367–372.
8. **Herraiz-Martínez FJ, Zamora G, Paredes F and Bonache J** (2011) Multiband printed monopole antennas loaded with OCSRRs for PANs and WLANs. *IEEE Antennas and Wireless Propagation Letters* **10**, 1528–1531.
9. **Long S and Walton M** (1979) A dual-frequency stacked circular-disc antenna. *IEEE Transactions on Antennas and Propagation* **27**(2), 270–273.
10. **Khan MU and Sharawi MS** (2014) Isolation improvement using an MTM inspired structure with a patch-based MIMO antenna system. In *The 8th European Conference on Antennas and Propagation (EuCAP 2014), The Hague*, 2718–2722.
11. **Sharawi MS, Khan MU, Numan AB and Aloi DN** (2013) A CSRR loaded MIMO antenna system for ISM band operation. *IEEE Transactions on Antennas and Propagation* **61**(8), 4265–4274.
12. **Ramachandran A, Mathew S, Viswanathan VP, Pezholil M and Kesavath V** (2016) Diversity-based four-port multiple input multiple output antenna loaded with interdigital structure for high isolation. *IET Microwaves, Antennas & Propagation* **10**(15), 1633–1642.
13. **Ramachandran A, Valiyaveettil Pushpakaran S, Pezholil M and Kesavath V** (2016) A four-port MIMO antenna using concentric square-ring patches loaded with CSRR for high isolation. *IEEE Antennas and Wireless Propagation Letters* **15**, 1196–1199.
14. **Luo Y, Chu QX, Li JF and Wu YT** (2013) A planar H-shaped directive antenna and its application in compact MIMO Antenna. *IEEE Transactions on Antennas and Propagation* **61**(9), 4810–4814.
15. **Liao WJ, Hsieh CY, Dai BY and Hsiao BR** (2014) Inverted-F/slot integrated dual-band four-antenna system for WLAN Access Points. *IEEE Antennas and Wireless Propagation Letters* **14**, 847–850.
16. **MoradiKordalivand A, Rahman TA and Khalily M** (2014) Common elements wideband MIMO antenna system for WiFi/LTE access-point applications. *IEEE Antennas and Wireless Propagation Letters* **13**, 1601–1604.
17. **Sonkki M, Pfeil D, Hovinen V and Dandekar KR** (2014) Wideband planar four-element linear antenna array. *IEEE Antennas and Wireless Propagation Letters* **13**, 1663–1666.

18. **Herraiz-Martínez J, García-Muñoz LE, Gonzalez-Ovejero D, Gonzalez-Posadas V and Segovia-Vargas D** (2009) Dual-frequency printed dipole loaded with split ring resonators. *IEEE Antennas and Wireless Propagation Letters* **8**, 137–140.

19. **Wang H, Liu L, Zhang Z, Li Y and Feng Z** (2015) A wideband compact WLAN/WiMAX MIMO antenna based on dipole with V-shaped ground branch. *IEEE Transactions on Antennas and Propagation* **63**(5), 2290–2295.

20. **Sharawi MS, Ikram M and Shamim A** (2017) A two concentric slot loop based connected array MIMO antenna system for 4 G/5 G terminals. *IEEE Transactions on Antennas and Propagation* **99**, 1–1.

21. **Kumar A, Ansari AQ, Kanaujia BK and Kishor J** (2018) High isolation compact four-port MIMO antenna loaded with CSRR for multiband applications. *Frequenz* **72**(9–10), 415–427.

22. **Dash JC and Sarkar D** (2022) A four-port CSRR-loaded dual-band MIMO antenna with suppressed higher order modes. *IEEE Access* **10**, 30770–30778.

23. **Montero-de Paz J, Ugarte-Munoz E, Herraiz-Martinez FJ, Gonzalez-Posadas V, Garcia-Munoz LE and SegoviaVargas D** (2011) Multi-frequency self-diplexed single patch antennas loaded with split ring resonators. *Progress In Electromagnetics Research* **113**, 47–66.

24. **Herraiz-Martínez FJ, Paredes F, Zamora G, Martin F and Bonache J** (2012) Dual-band printed dipole antenna loaded with open complementary split-ring resonators for wireless applications. *Microwave and Optical Technology Letters* **54**(4), 1014–1017.

25. **Caloz C, Itoh T and Rennings A** (2008) CRLH metamaterial leaky wave and resonant antennas. *IEEE Antennas and Propagation Magazine* **50**(5), 25–39.

D. Rajesh Kumar was born in Madurai, Tamilnadu, India, in 1987. He obtained the B.E. degree in electronics and communication engineering from Anna University, Tamilnadu, India, in 2008 and M.E. degree in communication systems from Anna University, Tamilnadu, India, in 2013. He has 9 years of teaching experience as assistant professor in SACSMAVMM Engineering College, Madurai, India. Currently, he is working as an Assistant Professor in the Department of ECE, Vel Tech Rangarajan Dr. Sagunthala R&D Institute of Science and Technology, Chennai, Tamilnadu, India. His research areas include mobile phone antenna design and RF system design.

T. Sangeetha was born in Madurai, Tamilnadu, India, in 1987. She obtained the B.E. degree in electronics and communication engineering from Anna University, Tamilnadu, India, in 2008 and M.E. degree in communication systems from Thiagarajar College of Engineering, Tamilnadu, India, in 2010. She completed her Ph.D. in the discipline of information and communication engineering in Anna University, Chennai. She has 10 years of teaching experience as assistant professor in SACSMAVMM Engineering College, Madurai, India. Currently, she is working as an Assistant Professor in Karpaga Vinayaga College of Engineering and Technology, Tamilnadu, India. Her research areas include microwave and RF antenna design.

K. G. Sujanth Narayan was born in Chennai, Tamilnadu, India, in 1996. He obtained the B.E. degree in electronics and communication engineering from R.M.K. Engineering College, Kavarapettai, Tamilnadu, and M.Tech. degree in communication systems from SASTRA Deemed University, Thanjavur, Tamilnadu, in the years 2017 and 2019, respectively. Currently, he is working as a research assistant and pursuing Ph.D. in the area of antennas and RF system design from School of Electrical and Electronics Engineering, SASTRA Deemed University, Thanjavur, Tamilnadu. He is a member of IEEE. His research areas include antennas, electromagnetics, RF system design, EMI/EMC, and vehicular communication.

G. Venkat Babu is Senior Assistant Professor in the Department of Electronics and Communication, SEEE, SASTRA Deemed University, Tamilnadu, India. He obtained the B.E. degree in electronics and communication from Bharathidasan University, Trichy, M.E. degree in microwave communication and radar from Dr. B.R. Ambedkar University, Agra, India, and Ph.D. in electronics and communication from Bhagwant University, Ajmer, India. His research is related to reconfigurable antenna and RF-MEMS. He has academic and research experience of about 19 years. He has published his research work in reputed journals and international and national conferences. He co-authored a book in the area of electromagnetic fields. He is a member of IEEE (Society APS & MTS) and life member of IETE and ISTE.

V. Prithivirajan received his B.E. degree in electronics and communication engineering from Anna University, Chennai, India, in 2006 and M.E. degree in communication systems from Anna University, India, in 2009. He completed his Ph.D. from the Department of Information and Communication, Anna University Chennai, India, in 2015. Currently, he is working as an Associate Professor at Vel Tech Rangarajan Dr. Sagunthala R&D Institute of Science and Technology, Chennai, Tamilnadu, India. His areas of interest are antennas and microwave filters using planar defected ground structure.

M. S. K. Manikandan is from the Department of Electronics and Communication Engineering, Thiagarajar College of Engineering, Madurai, India. He received the B.E. degree in electronics and communication engineering from NIT Trichy, Tamilnadu, India, in 1998 and ME degree in communication systems from Thiagarajar College of Engineering, Tamilnadu, India, in 2000. He completed Ph.D. in information and communication at Anna University, Tamilnadu, India, in 2010. Since 2001 he has been a faculty with electronics and communication engineering department, Thiagarajar College of Engineering. He is the author of more the 35 articles in reputed journals and conferences. His research interests include wireless communication and medical image analysis.